Journal of Interdisciplinary Mathematics
ISSN: 0972-0502 (Print), ISSN: 2169-012X (Online)
Vol. 27 (2024), No. 5, pp. 1053–1065
DOI : 10.47974/JIM-1932

Soret-driven influence on unsteady magnetohydrodynamic mixed oscillatory flow in a two-phase channel : Exploring the thermal effects

S. Kesavarani [†]
S. Lakshmi Priya*
Department of Mathematics and Statistics
Faculty of Science and Humanities
SRM Institute of Science and Technology
Kattankulathur 603203
Chennai
Tamil Nadu
India

Abstract

This research delves deeply into the intricate dynamics of the Soret effect within an unstable magnetohydrodynamic (MHD) mixed oscillatory flow occurring in a two-phase channel. The investigation spans a comprehensive spectrum of influences, including thermal, electrical, and chemical aspects. A pivotal aspect of this study involves the transformation of the governing equations into a dimensionless system, allowing for a nuanced examination of various media types, temperatures, and humidity levels within the specified research parameters. Subsequently, a rigorous analysis is conducted by applying the perturbation method to solve the equations. Through the utilization of illustrative charts, this study facilitates the computation of essential variables such as density and temperature. Furthermore, it delves into key parameters such as Gr, Gc, Sc, Sr, and others that characterize the flowing water.

Subject Classification: *76-10, 35G15, 34A34, 76D55, 76E25.*

Keywords: *Two-phase, Magnetohydrodynamics, Planar channels, Oscillating flows.*

1. Introduction

The application of fluid dynamics in magnetohydrodynamic (MHD) oscillating flow within two-phase systems holds practical significance

[†] *E-mail:* ks0756@srmist.edu.in
* *E-mail:* lakshmis3@srmist.edu.in (Corresponding Author)

© Taru Publications

across diverse fields such as engineering and agriculture. This encompasses a broad spectrum of considerations, including heat transfer, mass transfer, and chemical reactions. In practical terms, the fluid circulates through two-phase channels, serving as a conduit for the exchange of heat, air, and various chemicals. This versatile utilization finds relevance in a range of applications, contributing to advancements in engineering practices and agricultural processes.

In the realm of thermal dynamics, Muthucumaraswamy. R [1] delves into the intricacies of temperature variations, showcasing their susceptibility to homogeneous oscillations aligned with the initial reaction. In recent times, Mohammed Almakki [2] discussed the Entropy generation in MHD flow of viscoelastic nanofluids with homogeneous-heterogeneous reaction, partial slip and nonlinear thermal radiation. Recent investigations by Rehab Ali Shaban [3] focused on understanding the intricate dynamics of synovial fluid flow within porous layers, employing innovative double ZZ transformation techniques. Debasish Dey [4] delved into the realm of magnetohydrodynamic (MHD) fluid flow, specifically exploring the phenomenon of dual solutions in the context of heat and mass transfer across exponentially shrinking/stretching surfaces in porous media. Meanwhile, Y. Khan [5] delved into the nuanced realm of micropolar nanofluids, investigating the intriguing interplay between double diffusion, MHD flow, and slip boundary conditions, thus shedding light on previously unexplored aspects of fluid behavior. Amar B. Patil, [6] contributed to this body of research by analyzing the time-dependent behavior of MHD Prandtl nanofluids over linear stretching sheets, introducing convective boundary conditions into their study to capture more realistic scenarios. Sushil Yadav, Mukesh Kumar, Virendra Kumar [7] analysed resonance using perturbation technique. Furthermore, Medisetty Padma Devi and Suripeddi Srinivas [8] delved into the complex interplay between heat transfer effects and oscillatory MHD flow within porous channels, offering valuable insights into the fundamental mechanisms governing such systems. A Faque Ahmed Bhutto [9] further expanded the horizon of understanding by investigating the impact of oscillating streams on heat transfer within viscous MHD fluid flows, contributing to the development of more accurate predictive models for practical applications. Wei Zeng and Qian Wang [10] proposed an innovative numerical method aimed at resolving the challenging issue of oscillations in ideal magnetohydrodynamic equations, thereby enhancing the accuracy and reliability of computational simulations in this field. Lastly, Kirti Malviya [11] conducted a comprehensive heat transfer analysis

of MHD oscillatory hybrid nanofluid flows, highlighting the potential of such fluids in various engineering applications. Naufal Shyma Hussein, Rao Ganga Rama Koteswara, Velmurugan V, Sengan Sudhakar, Bommisetti Ravikumar, Dhadheech Pankaj,[12] have analysed the Advancing viscoelastic material modeling: Tackling time-dependent behavior with fractional calculus. These collective efforts represent significant strides in advancing our understanding of magnetohydrodynamic fluid flow phenomena, paving the way for further innovations and applications in this interdisciplinary field. This comprehensive exploration involves a detailed examination of their trajectory through temperature graphs, elucidating the intricate dynamics at play. Furthermore, the study delves into the consequential effects of chemical reactions on magnetohydrodynamic (MHD) oscillating flows, shedding light on the interplay between thermal characteristics and fluid behaviour. Through this meticulous analysis, the research contributes valuable insights into the thermal properties of optically dilute liquids, offering a nuanced understanding of their behaviour and the associated implications for MHD oscillating flows.

Nevertheless, current reviews fall short of providing a thorough examination of oscillating fluxes across diverse processes at different temperature ranges. Consequently, this article endeavours to fill this gap by scrutinizing the influence of a thin fluid on magnetohydrodynamic (MHD) oscillating shear instability within high-temperature processes. The study not only comprehensively explores but also elucidates and discusses solutions for ambient, heat, thermal, and air energy. Through this focused investigation, the research aims to contribute valuable insights into the intricate dynamics of MHD oscillations in high-temperature environments, offering comprehensive solutions and explanations across various energy domains.

2. Formulation of Problem

In the context of the Soret effect, we put forth a novel correlation between mixed convective shear flows in a porous medium characterized by unstable conductors and the oscillating dynamics of heat and chemicals. Introducing a magnetic field with a specified magnitude, denoted as B0, we observe its impact on both the buoyancy effect and the Soret effect along the Y-axis within the thermal solution. This unique configuration enables a nuanced exploration of the intricate interplay among convective shear, conductive instability, and the Soret effect. Through this, we aim to

provide a comprehensive understanding of the complex dynamics governing this system. By unraveling the connections between these factors, our research contributes valuable insights into the intricate relationships that shape the behavior of mixed convective shear flows in porous media with unstable conductors, shedding light on the underlying mechanisms at play in this intricate interplay of thermal, magnetic, and chemical influences.

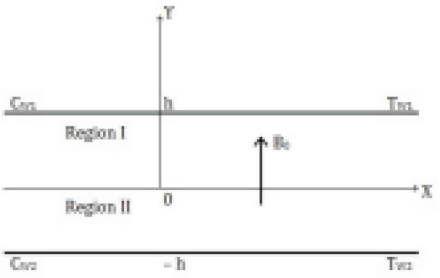

3. Motion to the governing equation for Region I and II:

$$\frac{\partial v'}{\partial yi'} = 0 \tag{1}$$

$$\frac{\partial U'}{\partial ti'} = -\frac{1}{\rho}\frac{\partial P'}{\partial x'} + \frac{v\partial^2 u}{\partial yi^2} + g\beta(T' - T_1') + g\beta'(C' - C_1') - \frac{v}{k'}U' - \frac{\sigma B_0^2}{\rho}U' - v'\frac{\partial U'}{\partial yi'} \tag{2}$$

$$\frac{\partial U'}{\partial ti'} = \frac{K}{\rho C_P}\frac{\partial^2 T'}{\partial yi^2} - \frac{1}{\rho}\frac{\partial q_1'}{\partial yi'}g + \frac{Q(T' - T'_1)}{\rho C_p} - v\frac{\partial T}{\partial yi} \tag{3}$$

$$\frac{\partial C'}{\partial ti'} = \frac{D\partial^2}{\partial yi^2} - \frac{K_1'(C' - C_1')}{d} - v'\frac{\partial C'}{\partial yi'} + \frac{D_{k_7}}{T}\frac{\partial^2 T'}{\partial yi^2} \tag{4}$$

Where $v' = -v_0(1 + \varepsilon e^{inx})$ is suction velocity, (Where i=1,2)

Boundary conditions:

$$U' = L_1\frac{\partial u'}{\partial yi'}, T' = T_1' + \delta_r^+\frac{\partial T'}{\partial yi'}, C' = C_1'\delta_c^+\frac{\partial C'}{\partial yi'} \text{ at } yi = 0 \tag{5}$$

$$U' = 0, T' = T_2' + \delta_t', C' = C_2'\delta_C'\frac{\partial C'}{\partial yi'} \text{ at } yi = d \tag{6}$$

(Where i=1,2)

4. The non-dimensional quantities

$$x=\frac{x'}{d},\ yi=\frac{y}{d},\ P=\frac{dP'}{\mu U_0},\ v=\frac{T'-T_1'}{T_2'-T_1'},\ \phi=\frac{C'-C_1'}{C_2-C_1},\ ti=\frac{U_0 ti'}{d},R_e=\frac{U_0 d}{v},\gamma=\frac{k}{d^2},$$
$$M=\frac{\sigma B_0^2 d^2}{\mu},G_r=\frac{g\beta(T_2-T_1)d^2}{vU_0},\ G_c=\frac{g\beta'(C_2-C_1)d^2}{vU_0},\ R=\frac{4I'd^2}{\mu},\ P_e=\frac{PC_pU_0d}{K},\ S_c=\frac{D}{Ud},$$
$$K_r=\frac{K_r'}{U_0},\ d_1=\frac{\delta_e'}{d},K'=Kd^2,\ S_r=\frac{D_k}{T}\frac{(T_\infty-T_\infty)}{(C_\infty-C_\infty)}$$

(Where i=1,2)

The basic equations (2) to (4) can be written as,

$$\mathrm{Re}\frac{\partial U}{\partial ti}=-\frac{\partial P}{\partial xi}+\frac{\partial^2 U}{\partial yi^2}+\lambda_1\frac{\partial U}{\partial yi}+G_r\theta+G_c\phi-\left(M+\frac{1}{K}\right)U \tag{9}$$

$$Pe\frac{\partial\theta}{\partial ti}=\frac{\partial^2\theta}{\partial yi^2}+Pe\lambda_2+(C_pR+\alpha)\theta \tag{10}$$

$$\frac{\partial\phi}{\partial ti}=S_C\frac{\partial^2}{\partial yi^2}+\lambda_3\frac{\partial\phi}{\partial yi}-K_r\phi+S_r\frac{\partial^2\phi}{\partial yi^2} \tag{11}$$

(Where i=1,2)

5. The boundary conditions: (t>0)

$$U_0=\gamma\frac{\partial U_0}{\partial yi},\theta_0=d_2\frac{\partial\theta_0}{\theta_0 yi},\phi_0=1+d_1\frac{\partial\phi_0}{\partial yi}\ \mathrm{at}\ yi=0 \tag{12}$$

$$U_0=0,\theta_0=1+d_2\frac{\partial\theta_0}{\partial yi},\phi_0=1+d_1\frac{\partial\phi_0}{\partial yi}\ \mathrm{at}\ yi=1 \tag{13}$$

(Where i=1,2)

6. Solution to the problem:

To obtain the equation (9) to (11) by using the boundary conditions (12) & (13) oscillatory flow.

$$U_1(y,t)=U_{10}(y)e^{iex} \tag{14}$$

$$\theta_1(y,t)=\theta_{10}(y)e^{iex} \tag{15}$$

$$\phi_1(y,t)=\phi_{10}(y)e^{iex} \tag{16}$$

$$-\frac{\partial P}{\partial x} = e^{iex_1} \tag{17}$$

$$U_2(y,t) = U_{20}(y)e^{iex} \tag{18}$$

$$\theta_2(y,t) = \theta_{20}(y)e^{iex} \tag{19}$$

$$\phi_2(y,t) = \phi_{20}(y)e^{iex} \tag{20}$$

$$-\frac{\partial P}{\partial x} = e^{iex_2} \tag{21}$$

Substitution of the equation (14) and (17) to equations (9) and (13) For i=1 and (18) and Substitution of the equation (21) to equations (9) and (13) for i=2,

$$U_1''(y) + a_1 U_1'(y) - a_2 U = -(\lambda + G_r v_1 + G_{C\phi 1}) \tag{22}$$

$$\theta_1''(y) + a_5 v_1'(y) - a_2 v_1 = 0 \tag{23}$$

$$\phi_1'(y) + \frac{\lambda_3}{S_C}\phi' - \left(\frac{K_r+\omega}{S_C}\right)\phi = \frac{S_r}{S_C}(A_{5e^{m_5 y}n_5^2} + A_{6e^{n6y}n_6^2}) \tag{24}$$

$$U_2''(y) + b_1 U_1'(y) - b_2 U = -(\lambda + G_r v_2 + G_{C\phi 2}) \tag{25}$$

$$\theta_2''(y) + b_5 v_2'(y) - b_2 v_2 = 0 \tag{26}$$

$$\phi_2'(y) + \frac{\lambda_3}{S_C}\phi' - \left(\frac{K_r+\omega}{S_C}\right)\phi = \frac{S_r}{S_C}(B_{5e^{m_5 y}m_5^2} + B_{6e^{m6y}m_6^2}) \tag{27}$$

7. Boundary Condition:

$$U_i = \gamma u_0', \theta_i = d_2\theta_i', \phi_i = d_1\phi_i' \text{ at } y = 0 \tag{28}$$

$$U_i = 0, \theta_i = 1 + d_2\theta_i', \phi_i = d_1\phi_i' \text{ at } y = 1 \tag{29}$$

(Where i=1,2) **Solution to velocity, temperature and concentration are obtained as,**

Region I:

$$U_{10}(y,t) = A_1 e^{n_1 y} + A_2 e^{n_2 y} + K_1 + K_2 e^{n_5 y} + K_3 e^{n_6 y} + K_4 e^{n3 y} + K_5 e^{n_4 y}$$

$$U_{11}(y,t) = A_7 e^{n_1 y} + A_8 e^{n_2 y} + K_1 + K_2 e^{n_5 y} + K_3 e^{n_6 y} + K_4 e^{n3 y} + K_5 e^{n_4 y}$$

$$\theta_{10}(y,t) = A_5 e^{n_5 y} + A_6 e^{n_6 y}$$

$$\theta_{11}(y,t) = A_{11} e^{n_5 y} + A_{12} e^{n_6 y}$$

$$\phi_{10}(y,t) = A_3 e^{n_3 y} + A_4 e^{n_4 y} - \frac{S_r}{S_C} K_{21} e^{n_5 y} - \frac{S_r}{S_C} K_{22} e^{n_6 y}$$

$$\phi_{11}(y,t) = A_9 e^{n_3 y} + A_{10} e^{n_4 y} - \frac{S_r}{S_C} K_{21} e^{n_5 y} - \frac{S_r}{S_C} K_{22} e^{n_6 y}$$

Region II:

$$U_{20}(y,t) = B_1 e^{m_1 y} + B_2 e^{m_2 y} + L_1 + L_2 e^{m_5 y} + L_3 e^{m_6 y} + L_4 e^{m3 y} + L_5 e^{m_4 y}$$

$$U_{21}(y,t) = B_7 e^{m_1 y} + B_8 e^{m_2 y} + L_1 + L_2 e^{m_5 y} + L_3 e^{m_6 y} + L_4 e^{m3 y} + L_5 e^{m_4 y}$$

$$\theta_{20}(y,t) = B_5 e^{m_5 y} + B_6 e^{m_6 y}$$

$$\theta_{21}(y,t) = B_{11} e^{m_5 y} + B_{12} e^{m_6 y}$$

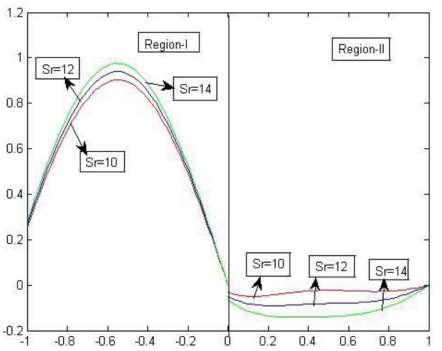

Figure 1

Soret Effect for velocity

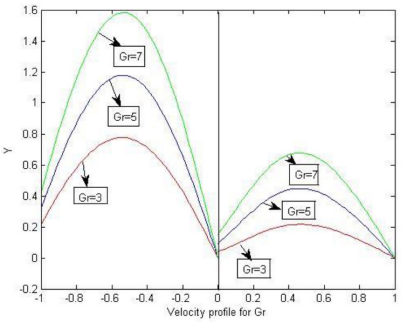

Figures 2

Grashof number for velocity

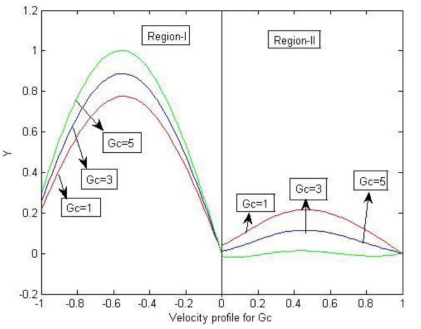

Figures 3

Grashof number for velocity

$$\phi_{20}(y,t) = B_3 e^{m_3 y} + B_4 e^{m_4 y} - \frac{S_r}{S_C} L_{21} e^{m_5 y} - \frac{S_r}{S_C} L_{22} e^{m_6 y}$$

$$\phi_{21}(y,t) = B_9 e^{m_3 y} + B_{10} e^{m_4 y} - \frac{S_r}{S_C} L_{21} e^{m_5 y} - \frac{S_r}{S_C} L_{22} e^{m_6 y}$$

8. Result and discussions:

Figure 1-3 vividly demonstrates the impact of the Soret effect (Sr) on velocity dynamics. Across various Sr values, the velocity undergoes a discernible increase in Region-I, followed by a gradual decrease in Region-II. This observed trend provides a nuanced insight into the intricate relationship between the Soret effect and velocity fluctuations. The variations in Sr values offer a comprehensive perspective on how this

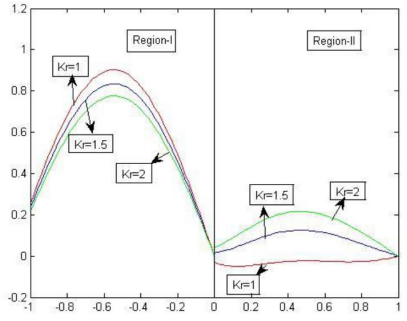

Figures 4

Effects of Kr for velocity

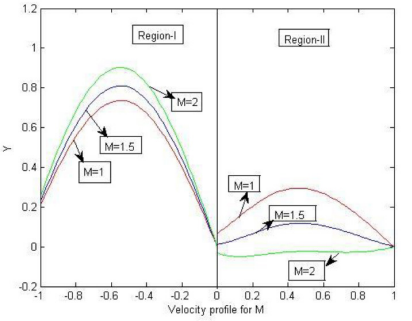

Figures 5

Effect of M for Velocity

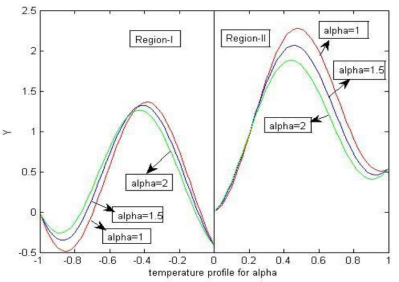

Figures 6

Effect of Alpha for Temperature

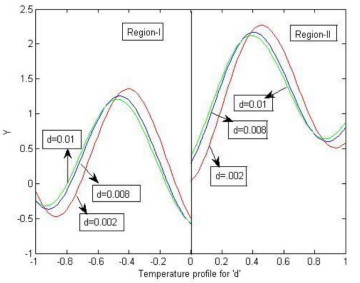

Figures 7

Effect of d for Temperature

influential factor influences the velocity profile, showcasing a dynamic interplay that unfolds distinctly in different regions. This analysis contributes to a deeper understanding of the intricate mechanisms governing the influence of the Soret effect on velocity within the specified context.

The influence of the Grashof number on heat and mass transfer was examined within the velocity field, revealing an initial ascent in Region-I succeeded by a gradual descent in Region-II. Throughout these analyses, all other parameters in the diagrams are maintained at constant values, allowing for a focused observation of the Grashof number's distinct impact on the dynamic interplay between heat and mass transfer in the specified regions. This approach enhances our understanding of the nuanced variations in the velocity field, emphasizing the consequential effects of the Grashof number on the intricate processes of heat and mass transfer.

This investigation highlights the discernible effects of Kr (chemical reaction) and M (Magnetic) on the velocity field within a porous medium, revealing a notable overall increase. The interplay of these parameters contributes to a dynamic enhancement of the velocity field, showcasing a comprehensive understanding of their combined influence. Through a systematic examination, it becomes evident that both chemical reaction (Kr) and magnetic effects (M) synergistically contribute to the observed acceleration in the velocity field. This nuanced analysis sheds light on the intricate relationships governing the porous medium's behavior, providing valuable insights into the collaborative impact of chemical reactions and magnetic forces on the overall velocity dynamics. Figures 4 and 5 represents the effects of Kr for velocity and Effects of M for velocity respectively.

The investigation centres on the Soret effect within the temperature and concentration fields, where diverse values of alpha and R play a

significant role. These varying parameters collectively induce an upward trend in Region I, succeeded by a gradual decline in Region II within the temperature field across two channels. This nuanced exploration delves into the complex interplay of alpha and R, revealing their considerable influence on the observed temperature dynamics. The systematic examination of different values contributes to a comprehensive understanding of the Soret effect's impact, unravelling the distinct patterns manifested in Regions I and II. This analysis provides valuable insights into the intricate relationships governing temperature variations across channels, particularly under the influence of the Soret effect and the associated parameters alpha and R. Effects of Alpha, D and M for temperature are given Figures 6, 7 and 8 respectively.

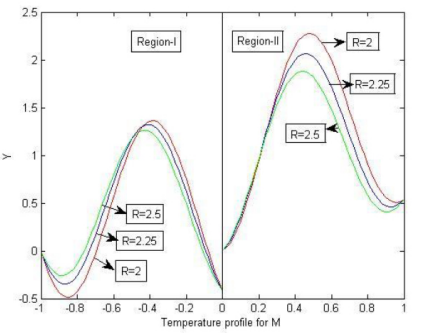

Figures 8

Effect of M for Temperature

This inquiry delves into the repercussions of elevating the Darcy number (Da) on the temperature field, exposing a notable upsurge in

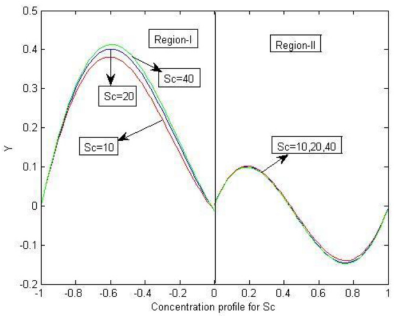

Figures 9

Effect of Sc for Concentration

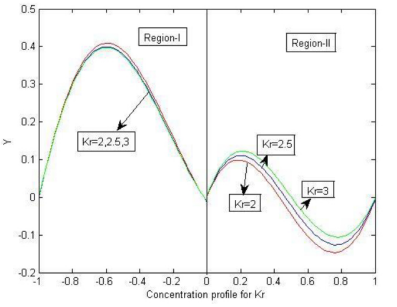

Figures 10

Effect of Kr for Concentration

Region I, succeeded by a subtle decline in Region II. The systematic exploration of the escalating Darcy number unveils a discernible influence on the temperature dynamics. The observed pattern illustrates an intensified temperature trend in Region I, followed by a modest attenuation in Region II. Through this thorough investigation, we gain deeper insights into the nuanced impact of varying Darcy numbers on the temperature field, elucidating the distinctive temperature variations across Regions I and II under the evolving influence of Da.

Delve into the effects of different values of Sc and Kr on concentration. The results show an increase in Region I and a decrease in Region II, highlighting an increment in concentration in the two-phase channel. Effects of Sc and Kr for concentration are given in Figures 9 and 10 respectively.

9. Conclusion

In unraveling the intricacies of the system, numerical solutions were employed to elucidate the velocity field across a range of parameters, including Gr, Gc, M, Kr, and Sr. The resultant outcomes were visually presented through illustrative graphics, offering a comprehensive depiction of the system's behavior under diverse conditions. Special attention was dedicated to scrutinizing the influence of the Soret effect on both the temperature and concentration fields, unraveling its impact through a meticulous analysis.

Expanding its focus, this investigation observed the dynamic responses of alpha, Da, R, Sc, and Kr, revealing their varied effects on the temperature and concentration fields. The recorded values showcased discernible elevations in both domains, and these intricate relationships were thoughtfully represented through visually compelling depictions. In essence, this numerical exploration not only enriches our comprehension of the system's behavior under different parameters but also provides a visual narrative of the nuanced interplay between Soret-driven effects and the broader thermodynamic characteristics within the studied framework.

References

[1] Muthucumaraswamy. R and Meenakshi Sundaram. S. Appl. Mech., vol. 33, No. 3, pp.245-257 (2006).

[2] Mohammed Almakki, Hiranmoy Mondal, Precious Sibanda, " Entropy Generation in MHD Flow of Viscoelastic Nanofluids with Homogeneous-Heterogeneous Reaction, Partial Slip and Nonlinear Thermal Radiation", *Journal of Thermal Engineering*, April, Year: 2020, Volume: 6, Issue: 3, pp : 327-34 (APR 2020).

[3] Rehab Ali Shaban, Enas Yahya Abdullah & Athraa Neamah Albukhuttar, "Study unsteady flow of synovial fluid in the elastic porosity of layers using double ZZ transformation", *Journal of Interdisciplinary Mathematics*, Volume 25, Issue 6 2022 ().

[4] Debasish Dey, O. D. Makinde & Rupjyoti Borah. "Analysis of Dual Solutions in MHD Fluid Flow with Heat and Mass Transfer Past an Exponentially Shrinking/Stretching Surface in a Porous Medium", *International Journal of Applied and Computational Mathematics*, Volume 8, article number 66, (2022).

[5] Y. Khan, Afraz Hussain Majeed, Muhammad Afraz Rasheed, A. Alameer, "Dual solutions for double diffusion and MHD flow analysis of micropolar nanofluids with slip boundary condition", Statistical and Computational Physics Volume 10 published in the year 2022 |https://doi.org/10.3389/fphy 2022.956737 .

[6] Amar B. Patil, Vishwambhar S. Patil, Pooja P. Humane, MD. Shamshuddin & Mehul A. Jadhav, "Double diffusive time-dependent MHD Prandtl nanofluid flow due to linear stretching sheet with convective boundary conditions", All Journals International Journal of Modelling and Simulation List of Issues, Volume 43, Issue 1, published on February 10th 2022 https://doi.org/10.1080/02286203.2022.2033499.

[7] Sushil Yadav, Mukesh Kumar, Virendra Kumar, "Analysis of Resonant Curve and Phase Portrait Due to Earth's Equatorial Ellipticity in the Earth-Moon System Using Perturbation Technique", Pages 275-298, Published online: 13 Nov 2022, Taru Publications. https://doi.org/10.1080/1726037X.2022.2120272.

[8] Medisetty Padma Devi, Suripeddi Srinivas, "Heat transfer effects on the oscillatory MHD flow in a porous channel with two immiscible

fluids", Nonlinear Analysis: Modelling and Control Vol. 28 No. 3 (2023).

[9] Afaque Ahmed Bhutto, Iftikhar Ahmed, Saeed Ahmed Rajput, "The effect of oscillating streams on heat transfer in viscous magnetohydrodynamic MHD fluid flow", VFAST Transactions on Mathematics, 11(1), 1-16. https://doi.org/10.21015/vem.v11/1.1386.

[10] Wei Zeng, Qian Wang, "A Locally Divergence-Free Oscillation-Eliminating Discontinuous Galerkin Method for Ideal Magnetohydrodynamic Equations", arXiv:2404.14274, https://doi.org/10 48550/arXiv 240414274 (2024).

[11] Kirti Malviya, Hanumagowda Bannihalli Naganagowda, Pavithra Kalluhole Matada, Sibbyala Vijay Kumar Varma, Chakravarthula SK Raju, Rohit Sharma, "Heat transfer analysis of MHD oscillatory SWCNT/MWCNT-H2O hybrid nanofluid flow in a channel", Journal of Applied Mathematics and Mechanics, (2024). https://doi.org/10.1002/zamm.202300366.

[12] Naufal Shyma Hussein, Rao Ganga Rama Koteswara, Velmurugan V, Sengan Sudhakar, Bommisetti Ravikumar, Dhadheech Pankaj, "Advancing viscoelastic material modeling: Tackling time-dependent behavior with fractional calculus", *Journal of Interdisciplinary Mathematics*, Volume 27, Issue 2, Pages 307 – 3162024 (2024). Taru Publications.

Received March, 2024